Inorg. Chem. **2005**, *44*, 2934–2943

Chromium(V) Complexes of Hydroxamic Acids: Formation, Structures, and Reactivities

Swetlana Gez, Robert Luxenhofer,† Aviva Levina, Rachel Codd,* and Peter A. Lay*

Centre for Heavy Metals Research and Centre for Structural Biology and Structural Chemistry, School of Chemistry, University of Sydney, NSW, 2006, Australia

Received November 29, 2004

A new family of relatively stable Cr(V) complexes, $[Cr^{V}O(L)_2]^-$ (LH_2 = RC(O)NHOH, R = Me, Ph, 2-HO–Ph, or HONHC(O)$(CH_2)_6$), has been obtained by the reactions of hydroxamic acids with Cr(VI) in polar aprotic solvents. Similar reactions in aqueous solutions led to the formation of transient Cr(V) species. All complexes have been characterized by electron paramagnetic resonance spectroscopy and electrospray mass spectrometry. A Cr(V) complex of benzohydroxamic acid (**1**, R = Ph) was isolated in a pure form (as a K^+ salt) and was characterized by X-ray absorption spectroscopy and analytical techniques. Multiple-scattering analysis of X-ray absorption fine structure spectroscopic data for **1** (solid, 10 K) point to a distorted trigonal-bipyramidal structure with trans-oriented Ph groups and Cr–ligand bond lengths of 1.58 Å (Cr–O), 1.88 Å (Cr–O(C)), and 1.98 Å (Cr–O(N)). Under ambient conditions, **1** is stable for days in aprotic solvents but decomposes within minutes in aqueous solutions (maximal stability at pH ∼ 7), which leads predominantly to the formation of Cr(III) complexes. Complex **1** readily undergoes ligand-exchange reactions with biological 1,2-diols, including D-glucose and mucin, in neutral aqueous solutions. It differs from most other types of Cr(V) complexes in its biological activity, since no oxidative cleavage of plasmid DNA in vitro and no significant bacterial mutagenicity (in the TA 102 strain of *Salmonella typhimurium*) was observed for **1**. In natural systems, stabilization of Cr(V) by hydroxamato ligands from bacterial-derived siderophores (followed by ligand-exchange reactions with more abundant carbohydrate ligands) may occur during the biological reduction of Cr(VI) in contaminated soils.

Introduction

Hydroxamic acid (RC(O)NHOH) moieties are widespread in biological systems (particularly in the microbial and plant kingdoms) as key functional groups of siderophores, which are relatively small biomolecules that are responsible for high-affinity scavenging of Fe(III) (and possibly of other transition metal ions) from the environment.[1] Strong binding of metal ions provides the basis for numerous applications of hydroxamic acids as pharmacological agents (inhibitors of metalloenzymes).[2] Metal binding to hydroxamic acids (1:1) usually occurs in a bidentate fashion (Scheme 1) with the formation of singly or doubly deprotonated (hydroxamato or hydroximato) ligands.[3,4] While coordination chemistry of hydroxamic acids has been studied extensively (particularly with Cu(II), Zn(II), Fe(III), Co(III), and Cr(III) ions),[3,4] there have been no reports in the literature on the formation of Cr(V) complexes of these ligands. The current interest in coordination chemistry of Cr(V) arises mainly from the proposed crucial role of reactive Cr(V) intermediates in Cr(VI)-induced genotoxicity and carcinogenicity.[5] Accumu-

Scheme 1. Common Modes of Binding of Hydroxamic Acids to Transition Metal Ions (M^{n+})[a]

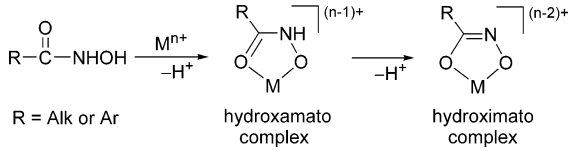

[a] References 3 and 4.

* To whom correspondence should be addressed. E-mail: r.codd@chem.usyd.edu.au, p.lay@chem.usyd.edu.au.

† Present address: Technische Universität München, Department Chemie, Lehrstuhl für Makromolekulare Stoffe, Lichtenbergstrasse 4, 85747 Garching, Germany.

(1) Miller, M. J. *Chem. Rev.* **1989**, *89*, 1563−1579.
(2) Muri, E. M. F.; Nieto, M. J.; Sindelar, R. D.; Williamson, J. S. *Curr. Med. Chem.* **2002**, *9*, 1631−1653.
(3) Kurzak, B.; Kozlowski, H.; Farkas, E. *Coord. Chem. Rev.* **1992**, *114*, 169−200.
(4) (a) Abu-Dari, K.; Ekstrand, J. D.; Freyberg, D. P.; Raymond, K. N. *Inorg. Chem.* **1979**, *18*, 108−112. (b) Abu-Dari, K.; Raymond, K. N. *Inorg. Chem.* **1980**, *19*, 2034−2040.

10.1021/ic048317d CCC: $30.25
Published on Web 03/19/2005

lation and reduction of Cr(VI) by microorganisms and plants, used for bioremediation of contaminated soils,[6] may well involve the interactions of Cr(VI) with hydroxamato moieties of siderophores.

This work presents the first description of Cr(V) intermediates formed during the reactions of Cr(VI) with hydroxamic acids. In a similar manner as described in previous studies on Cr(V) complexes,[7−10] a combination of electron paramagnetic resonance (EPR) spectroscopy, electrospray mass spectrometry (ESMS), and X-ray absorption spectroscopy (XAS) was used for the structural characterization of Cr(V) complexes, since they have not yet been crystallized due to their low stabilities in solutions.

Experimental Section

Caution! Cr(VI) compounds are human carcinogens,[11] and Cr(V) complexes are mutagenic and potentially carcinogenic;[5] appropriate precautions should be taken to avoid skin contact and inhalation of their solutions and dusts.

Reagents and Solutions. Commercial reagents of analytical or higher purity (purchased from Aldrich, Sigma, or Merck) were used without further purification. Hydroxamic acids, including acetohydroxamic acid (AHA), benzohydroxamic acid (BHA), salicylhydroxamic acid (SaHA), and suberohydroxamic acid (SuHA), were from Aldrich. Acetone and *n*-hexane (BP Chemicals) were distilled after boiling for 2−3 h with activated 4 Å molecular sieves (Aldrich). Water was purified by the Milli-Q technique. Model Cr(V) complexes, $Na[CrO(ehba)_2]\cdot 1.5H_2O$ ($ehbaH_2$ = 2-ethyl-2-hydroxybutanoic acid) and $[Cr(O)_2(phen)_2](BF_4)\cdot 0.3Et_2O$ (phen = 1,10-phenanthroline), were synthesized and characterized as reported previously.[10,12,13] Stock solutions of the buffers were treated by Chelex 100 chelating resin (BioRad) and stored at 4 °C. Working solutions of the buffers were prepared daily by adjusting the pH values of the stock solutions with high purity NaOH (99.99%, Aldrich); the pH values were measured by an Activon 210 ionometer with an AEP 321 glass/calomel electrode. Concentrations of the catalytic metals (Fe(III) and Cu(II)) in the buffers were <0.5 μM, as determined by Buettner's ascorbate method.[14]

Synthesis of $K[Cr^{V}O(L)_2]\cdot Me_2CO$ (1, LH_2 = BHA). Finely ground anhydrous $K_2Cr_2O_7$ (120 mg, 0.816 mmol Cr) and BHA (330 mg, 2.40 mmol) were dissolved with stirring (~30 min at 22 °C) in *N*,*N*-dimethylformamide (DMF) (10 mL), and the solution was kept at 22 °C for a further 5 h. To the resultant dark-brown solution, acetone (10 mL) was added, followed by the slow addition (~10 min, with stirring) of *n*-hexane (30 mL), which resulted in separation of a black oil. This oil was dissolved in a minimal volume of acetone, and the solution was applied to a column (1.5 × 20 cm) of Sephadex LH-20 (Amersham Biosciences). Elution of the column with acetone resulted in separation of a fast-moving green fraction (containing Cr(III)−BHA complexes, as shown by ESMS, see Results), which was discarded, followed by a brown fraction of **1**. A yellow fraction, probably containing unreacted Cr(VI), remained on the column. The brown fraction was collected, acetone was removed under reduced pressure (~30 °C), and the residue was dried under vacuum to a constant mass (3 days at 22 °C), leading to a brown-black microcrystalline powder (135 mg; yield of **1**, 38%). Anal. Calcd for $C_{17}H_{16}N_2O_6CrK$: C, 46.89; H, 3.70; N, 6.43; Cr, 11.94; K, 8.98. Found (average values and standard deviations for three different preparations of **1**): C, 46.5 ± 0.6; H, 3.8 ± 0.2; N, 4.8 ± 0.8; Cr, 11.8 ± 0.2; K, 9.5 ± 0.5. Thermogravimetric analysis: mass loss 14% at 25−140 °C. ESMS (acetone, −ve ion): 338.1 *m*/*z*. UV−vis (DMF): 740 nm (2.0×10^2 M^{-1} cm^{-1}). EPR (DMF): $g_{iso} = 1.9820$; $A_{iso}(^{53}Cr) = 13.9 \times 10^{-4}$ cm^{-1}; $a_N = 0.89 \times 10^{-4}$ cm^{-1} (quintet). Magnetic moment (solid, 295 K): $\mu_{eff} = 2.07$ μ_B. IR (KBr matrix): 3600−2500 m, br, 1710 m, 1600 m, 1543 s, 1494 m, 1445 m, 1420 m, 1373 sh, 1344 s, 1176 w, 1144 w, 1110 w, 1071 w, 1024 w, 977 m, 918 m, 775 w, 721 m, 696 s, 647 m, 550 m, br. The product is soluble (up to ~0.2 M) in polar aprotic solvents, such as acetonitrile (MeCN), DMF, or dimethyl sulfoxide (DMSO), and slightly soluble (~0.5 mM) in water at 22 °C. For preparation of aqueous solutions of **1** (0.20−1.0 mM), freshly prepared solutions in MeCN, DMF, or DMSO (20−100 mM) were diluted with H_2O or aqueous buffer solutions.

Analytical Techniques. The Cr content of **1** was determined (after digestion of the samples with 69% HNO_3) by C_2H_2/air flame atomic absorption spectroscopy, using a Varian SpecAA-800 spectrometer, calibrated with standard Cr(III) solutions (Aldrich). Determination of K^+ was performed with a Sherwood 410 flame photometer, using KCl as a standard. Elemental analyses (C, H, N) were performed by the Australian National University Microanalytical Unit or the Microanalysis Laboratory of the Chemistry Department, University of Otago (Dunedin, New Zealand). Thermogravimetric analyses (TGA) were performed on a TGA 2950 analyzer (TA Instruments) by heating the samples in an atmosphere of high purity N_2 (BOC gases) from 25 to 500 °C at 1 °C/min. Magnetic susceptibility was measured on a Sherwood Scientific magnetic balance, calibrated with $(NH_4)_2Fe(SO_4)_2\cdot 6H_2O$, and diamagnetic corrections for the constituent atoms were calculated from the literature.[15] Solid-state IR spectra were recorded using the diffuse reflectance technique (for the mixtures with KBr) on a BioRad FTS-40 spectrometer. Cyclic voltammetry experiments were performed using a Bioanalytical Systems BAS 100B Electrochemical Analyzer (scan rate, 100 mV s^{-1}; 100% *iR* compensation) with a glassy carbon working electrode (3 mm diameter), an Ag/AgCl reference electrode, filled with 3.0 M aqueous NaCl, Pt wire as an auxiliary electrode, and ferrocene (Fc) as an internal standard. Electrochemical measurements were carried out in DMF solutions, containing $(^nBu_4N)BF_4$ (0.10 M) as the supporting electrolyte, and saturated with O_2-free Ar (BOC gases). Electronic absorption spectra were acquired on a Hewlett-Packard HP 8452 A diode-array spectrophotometer (300−800 nm) or on a Varian Cary 5E spectrophotometer (700−1500 nm). Concentrations of Cr(VI) in the decomposition products of **1** were determined spectrophotometrically with diphenylcarbazide (DPC, $\epsilon = 4.2 \times 10^4$ M^{-1} cm^{-1} at 540 nm),[16] as described previously,[17] and calibrations were performed by a standard additions method.

(5) For a recent review, see: Levina, A.; Codd, R.; Dillon, C. T.; Lay, P. A. *Prog. Inorg. Chem.* **2003**, *51*, 145−250 and references therein.
(6) Zayed, A. M.; Terry, N. *Plant Soil* **2003**, *249*, 139−156.
(7) Codd, R.; Levina, A.; Zhang, L.; Hambley, T. W.; Lay, P. A. *Inorg. Chem.* **2000**, *39*, 990−997.
(8) Headlam, H. A.; Weeks, C. L.; Turner, P.; Hambley, T. W.; Lay, P. A. *Inorg. Chem.* **2001**, *40*, 5097−5105.
(9) Levina, A.; Zhang, L.; Lay, P. A. *Inorg. Chem.*, **2003**, *42*, 767−784.
(10) Weeks, C. L.; Levina, A.; Dillon, C. T.; Turner, P.; Fenton, R. R.; Lay, P. A. *Inorg. Chem.* **2004**, *43*, 7844−7856.
(11) *IARC Monographs on the Evaluation of the Carcinogenic Risk of Chemicals to Humans. Vol. 49. Chromium, Nickel and Welding*; International Agency on the Research of Cancer: Lyon, France, 1990.
(12) Krumpolc, M.; Roček, J. *J. Am. Chem. Soc.* **1979**, *101*, 3206−3209.
(13) Judd, R. J.; Hambley, T. W.; Lay, P. A. *J. Chem. Soc., Dalton Trans.* **1989**, 2205−2210.
(14) Buettner, G. R. *Methods Enzymol.* **1990**, *186*, 125−127.
(15) Mabbs, F. E.; Machin, D. J. *Magnetism and Transition Metal Complexes*; Chapman and Hall: London, 1973.

Solid-state and solution EPR spectra (X-band) were acquired on a Bruker EMX spectrometer, using quartz capillaries (solid state) and a Wilmad quartz flat cell (solutions); calibrations of the magnetic field and the microwave frequency were performed with an EMX 035 NMR gaussmeter and an EMX 048T microwave bridge controller, respectively. Low-temperature (77 K) EPR spectra were recorded using a "coldfinger" liquid N_2 dewar. Typical instrumental settings were as follows: center field, 3480 G; sweep width, 6900 G (solids) or 200 G (solutions); resolution, 1024 points; microwave power, 2.0 mW; microwave frequency, ~9.27 GHz (solids at 77 K), ~9.78 GHz (solids at 295 K), or ~9.67 GHz (solutions); modulation frequency, 100 kHz; modulation amplitude, 5.0 G (solids) or 0.40−1.0 G (solutions); time constant, 20.48 ms; receiver gain, 10^2-10^5; and number of scans, 5. The EPR spectra were processed with WinEPR and simulated with WinSim software, respectively;[18] second-order corrections were applied in the determinations of the g_{iso}, A_{iso}, and a_N values.

The ESMS analyses were performed using a Finnigan LCQ mass spectrometer; typical experimental settings were as follows: sheath gas (N_2) pressure, 60 psi; spray voltage, 4.0 kV; capillary temperature, 200 °C; cone voltage, 25 V; tube lens offset, 20 V; m/z range, 100−2000 (both in positive- and negative-ion modes; no significant signals were detected at $m/z > 1200$). Variations in the capillary temperature (150−220 °C) and cone voltage (3−40 V) did not cause significant changes in the spectra. Analyzed solutions (5 μL, ~1 mM Cr) were injected into a flow of H_2O/MeOH (1:1 v/v; flow rate, 0.20 mL min^{-1}). Acquired spectra were the averages of 10 scans (scan time, 10 ms). Simulations of the mass spectra were performed using IsoPro software.[19]

All the analytical results were reproduced in at least two independent experimental series, using different sets of stock solutions and different preparations of **1**; relative deviations in the results of parallel experiments did not exceed 10%.

X-ray Absorption Spectroscopy and Data Processing. The chromium K-edge spectrum of **1** was recorded on the Australian National Beamline Facility (beamline 20B) at the Photon Factory, Tsukuba, Japan. The beam energy was 2.5 GeV, and the beam current was 300−400 mA. A Si[111] double-crystal monochromator was detuned by 50%. The spectrum was recorded in transmission mode, using N_2/He-filled ionization chambers. A solid sample was mixed with boron nitride (BN, 1:1 w/w) and pressed into a 0.5-mm pellet supported in an Al spacer between two 63.5-μm Kapton tape windows. The sample temperature was maintained at 10 ± 1 K using a closed-cycle He CryoIndustries REF-1577-D22 cryostat. Collection of XAS data at low temperature minimized sample photodamage, improved the signal-to-noise ratio, and maximized the multiple-scattering contributions to the X-ray absorption fine structure (XAFS) spectrum.[20] The spectrum was averaged from three scans taken at different positions on the sample; no color changes at irradiated spots were observed, and the edge energies differed by <0.1 eV between the scans. The energy scale was calibrated using a Cr foil as an internal standard (calibration energy, 5989.0 eV, which corresponded to the first peak of the first derivative of Cr(0) edge).[21] Averaging, background subtraction, and the calculations of theoretical XAFS spectra were performed using the XFIT software package,[21] including FEFF 4.06[22] and FEFF 6.01[23] algorithms, as described previously.[20,24] The determinacies (N_i/p, where N_i is the number of independent observations and p is the number of varied parameters) of the models used in the single- and multiple-scattering (SS and MS) fits to the XAFS data were estimated by the method of Binsted et al.,[25] taking into account the applied restraints and constraints. Overdetermined models ($N_i/p > 1$) were used in XAFS calculations, which enabled meaningful fits to be obtained.[25] The goodness-of-fit parameters for XAFS fittings using different models were compared using a statistical F-test.[26,27] The random errors in the estimated XAFS parameters that arise from the noise in the data were determined by Monte Carlo analysis within the XFIT software.[21] Starting coordinate sets for MS XAFS calculations were obtained from molecular models of **1** built using the HyperChem software,[28] and geometric parameters of the ligands were taken from the crystal structures of Cr(III)−BHA complexes.[4]

Biological Activity Assays. The abilities of **1** and model Cr(V) complexes to induce oxidative DNA cleavage were determined from the decrease in the relative concentrations of form I (covalently closed supercoiled) DNA and increases in those of form II (nicked circular) and form III (linear) DNA. Methods for preparation of supercoiled plasmid pUC9 DNA (supplied by the laboratory of Dr. N. E. Dixon, Australian National University) and DNA cleavage assays were described previously (for the reactions of $[Cr^{V}O(ehba)_2]^-$).[29] The assays were performed in phosphate buffers (0.10 M, pH 7.4), since the use of organic buffers leads to inhibition of DNA cleavage by Cr(V) complexes.[29b] Determination of Cr−DNA binding caused by fresh and decomposed solutions of **1** was performed by a method developed for the reactions of DNA with $[Cr^{V}O(ehba)_2]$,[30] using Bio-Gel P-30 spin columns (Bio-Rad) for removal of unbound Cr complexes.[30] The Cr−DNA binding studies were performed in *N*-(2-hydroxyethyl)-piperazine-*N*′-(2-ethanesulfonate) (HEPES) buffer (0.10 M, pH 7.4), since the use of phosphate buffer leads to a competition for Cr binding with the phosphate groups of DNA.[30] The bacterial mutagenicity of **1** was tested using the TA102 strain of *Salmonella typhimurium*, as described previously for $[Cr^{V}O(ehba)_2]^-$ and other Cr(V) complexes.[31,32]

(16) *Standard Methods for the Examination of Water and Wastewater*, 19th ed.; American Public Health Association: Washington, DC, 1995; pp 3.59−3.60.

(17) Levina, A.; Bailey, A. M.; Champion, G.; Lay, P. A. *J. Am. Chem. Soc.* **2000**, *122*, 6208−6216.

(18) (a) *WinEPR, Version 960801*; Bruker-Franzen Analytic: Bremen, Germany, 1996. (b) Duling, D. R. *J. Magn. Reson.* **1994**, *B104*, 105−110. The WinSim software is available via the Internet at http://epr.niehs.nih.gov/.

(19) *IsoPro 3.0*; Senko, M.: Sunnyvale, CA, 1998.

(20) (a) Rich, A. M.; Armstrong, R. S.; Ellis, P. J.; Freeman, H. C.; Lay, P. A. *Inorg. Chem.* **1998**, *37*, 5743−5753. (b) Rich, A. M.; Armstrong, R. S.; Ellis, P. J.; Lay, P. A. *J. Am. Chem. Soc.* **1998**, *120*, 10827−10836.

(21) (a) Ellis, P. J.; Freeman, H. C. *J. Synchrotron Radiat.* **1995**, *2*, 190−195. (b) *XFIT for Windows 95*; Australian Synchrotron Research Program: Sydney, Australia, 1996.

(22) Mustre de Leon, J.; Rehr, J. J.; Zabinsky, S. I.; Albers, R. C. *Phys. Rev. B* **1991**, *44*, 4146−4156.

(23) Rehr, J. J.; Albers, R. C.; Zabinsky, S. I. *Phys. Rev. Lett.* **1992**, *69*, 3397−3400.

(24) Levina, A.; Armstrong, R. S.; Lay, P. A. *Coord. Chem. Rev.* **2005**, *249*, 141−160.

(25) Binsted, N.; Strange, R. W.; Hasnain, S. S. *Biochemistry* **1992**, *31*, 12117−12125.

(26) Neville, A. M.; Kennedy, J. B. *Basic Statistical Methods for Engineers and Scientists*; International Textbook: Scranton, PA, 1966; pp 312−313.

(27) Levina, A.; Lay, P. A. *Inorg. Chem.* **2004**, *43*, 324−335.

(28) *HyperChem, Version 5.1*; Hypercube Inc.: Gainesville, FL, 1996.

(29) (a) Farrell, R. P.; Judd, R. J.; Lay, P. A.; Dixon, N. E.; Baker, R. S. U.; Bonin, A. M. *Chem. Res. Toxicol.* **1989**, *2*, 227−229. (b) Levina, A.; Barr-David, R.; Codd, R.; Lay, P. A.; Dixon, N. E.; Hammershøi, A.; Hendry, P. *Chem. Res. Toxicol.* **1999**, *12*, 371−381.

(30) Levina, A.; Lay, P. A.; Dixon, N. E. *Chem. Res. Toxicol.* **2001**, *14*, 946−950.

(31) Dillon, C. T.; Lay, P. A.; Bonin, A. M.; Dixon, N. E.; Collins, T. J.; Kostka, K. L. *Carcinogenesis* **1993**, *14*, 1875−1880.

Chart 1. Proposed Structures of Cr(V) Hydroximato Complexes

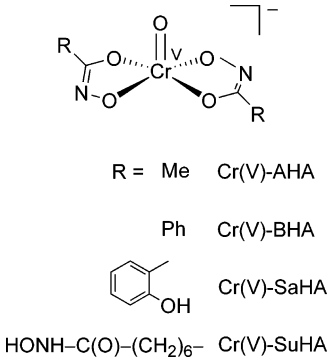

Results

Generation of Cr(V)−Hydroximato Complexes in Solutions. Reactions of hydroxamic acids (0.10 M of AHA, BHA, SaHA, or SuHA, Chart 1) with Cr(VI) (10 mM, from $K_2Cr_2O_7$) in polar aprotic solvents, such as DMF, DMSO, or MeCN, led to color changes from yellow to green or brown (within minutes or hours at 22 °C) and to the appearance of strong sharp signals in the solution EPR spectra ($g_{iso} \sim 1.982$, Figure 1 and Table 1), which are characteristic for Cr(V) complexes.[5,33] The spectra (Figure 1a,c) also possessed satellite signals due to the hyperfine splitting of the ^{53}Cr isotope (natural abundance, 9.55%). The A_{iso} values ($\sim 14 \times 10^{-4}$ cm^{-1}, Table 1) were typical for five-coordinate Cr(V) species.[5,33] Both the main signals and the ^{53}Cr satellites showed well-resolved quintet patterns (Figure 1b,c) due to the superhyperfine coupling of two equivalent ^{14}N nuclei ($a_N = (0.8-0.9) \times 10^{-4}$ cm^{-1}, Table 1). Similar, but much weaker, EPR signals were observed (Figure S1, Supporting Information) during the reactions of hydroxamic acids (0.10 M of AHA or BHA, or 25 mM of SaHA or SuHA) with Cr(VI) (Na_2CrO_4, 10 mM) in neutral aqueous solutions (0.10 M HEPES buffer, pH 7.4) in the presence of the most abundant biological reductant, glutathione (GSH, 10 mM),[34] or in weakly acidic aqueous solutions (0.10 M acetate buffer, pH 5.0) in the absence of added reductants. Maximal intensities of the EPR signals for aqueous solutions were achieved at ~3 min after mixing of the reagents, and the signals completely disappeared within ~30 min at 22 °C.

Formation of Cr(V) species during the reactions of Cr(VI) with hydroxamic acids could also be followed by electronic absorption (UV−vis) spectroscopy due to the appearance of a band at 700−800 nm that resulted from a *d*→*d* electronic transition (Figure S2a in Supporting Information), which is known to be specific for Cr(V) complexes.[35] Kinetic studies by UV−vis spectroscopy (reaction conditions corresponded to those in Figure 1) showed that the maximal

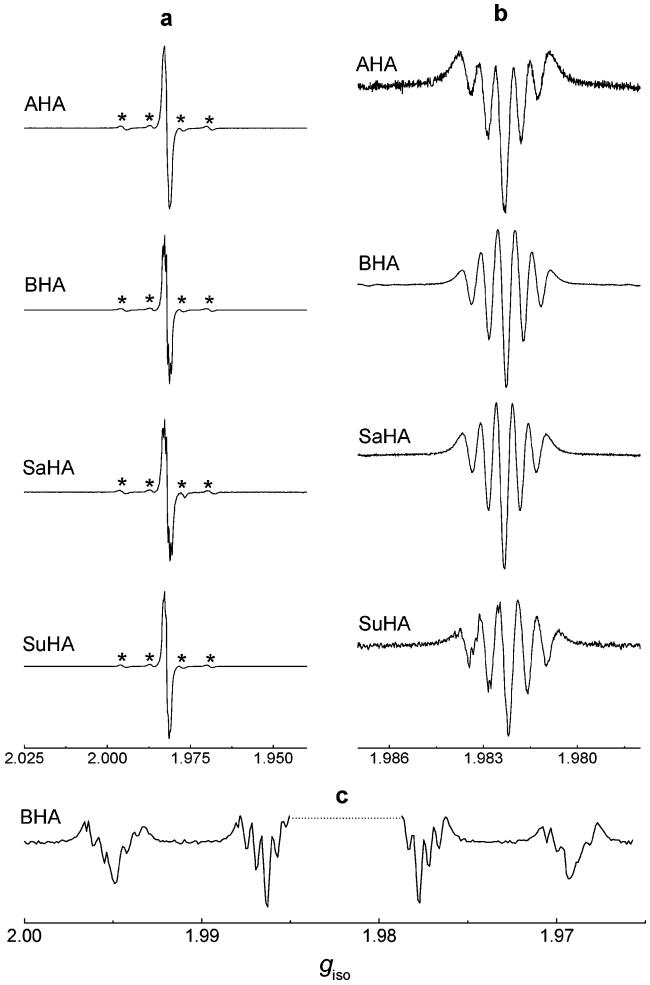

Figure 1. X-band EPR spectra (22 °C) of the solutions formed during the reactions of hydroxamic acids (0.10 M of AHA, BHA, SaHA, or SuHA) with Cr(VI) (10 mM, from $K_2Cr_2O_7$) in DMF for 3.5 h at 22 °C: (a) first-derivative spectra, modulation amplitude = 1.0 G (satellite signals due to ^{53}Cr hyperfine coupling are shown by asterisks); (b) second-derivative spectra (central signals only, modulation amplitude = 0.40 G); and (c) an expanded view of the satellite signals for the Cr(V)−BHA complex (second-derivative spectrum, modulation amplitude = 1.0 G; the central signal is removed for clarity).

concentrations of Cr(V) were achieved at 2, 4, 14, or >15 h (22 °C) for the reactions of SaHA, SuHA, BHA, or AHA, respectively; typical kinetic curves at 742 nm are shown in Figure S2b, Supporting Information. All the formed Cr(V) complexes, except for that of SaHA, were stable in DMF solutions for at least 15 h at 22 °C in the presence of excess Cr(VI) and the ligand; the signal due to the SaHA complex decayed significantly after ~2 h (Figure S2b). The kinetic data (Figure S2b) also indicated that the reactions of Cr(VI) with aromatic hydroxamic acids (BHA and SaHA) led to ~10-fold higher yields of Cr(V) complexes than the reactions with aliphatic ligands, AHA or SuHA (given that the absorbances at 742 nm were similar for all of the complexes). Studies of the reaction mixtures by ESMS (Figure S3 and Table S1 in the Supporting Information) revealed the formation of Cr(V) hydroximato complexes of the general formula $[Cr^{V}O(L)_2]^-$ (where LH_2 is a hydroxamic acid, m/z = −214.1, −338.1, −370.1, and −472.2 for AHA, BHA, SaHA, and SuHA, respectively), as well as of Cr(III)

(32) Dillon, C. T.; Lay, P. A.; Bonin, A. M.; Dixon, N. E.; Sulfab, Y. *Aust. J. Chem.* **2000**, *53*, 411−424.
(33) Barr-David, G.; Charara, M.; Codd, R.; Farrell, R. P.; Irwin, J. A.; Lay, P. A.; Bramley, R.; Brumby, S.; Ji, J.-Y.; Hanson, G. R. *J. Chem. Soc., Faraday Trans.* **1995**, *91*, 1207−1216.
(34) Kosower, E. M. In *Glutathione*: *Metabolism and Function*; Arias, I. M., Jacoby, W. B., Eds.; Raven Press: New York, 1976; pp 1−15.
(35) Farrell, R. P.; Lay, P. A. *Comments Inorg. Chem.* **1992**, *13*, 133−175.

Table 1. EPR Spectroscopic Parameters of Cr(V) Hydroximato Complexes in Solutions (22 °C)

complex	solvent	g_{iso}	A_{iso},[a] 10^{-4} cm^{-1}	a_N,[b] 10^{-4} cm^{-1}	LW,[c] 10^{-4} cm^{-1}
Cr(V)−AHA[d]	DMF	1.9822	13.9	0.86	1.0
Cr(V)−BHA[d]	DMF	1.9820	13.9	0.90	0.92
Cr(V)−SaHA[d]	DMF	1.9820	14.4	0.93	0.87
Cr(V)−SuHA[d]	DMF	1.9822	13.8	0.83	1.0
1[e]	DMSO	1.9820	13.8	0.88	0.88
1[e]	DMF	1.9820	13.9	0.89	0.95
1[e]	MeCN	1.9821	14.0	0.85	1.3
1[e]	acetone	1.9821	14.0	0.90	1.3
1[f]	H_2O	1.9819	14.4	0.82	1.0

[a] Hyperfine splitting due to the coupling of ^{53}Cr nuclei (relative abundance, 9.55%). [b] Superhyperfine splitting due to the coupling of ^{14}N nuclei. [c] Line width of the EPR signal. [d] Complexes were generated in situ by the reactions of Cr(VI) (10 mM, from $K_2Cr_2O_7$) with the corresponding hydroxamic acid (0.10 M) in DMF for 3.5 h at 22 °C. [e] The isolated complex **1** (1.0 mM) was dissolved in the corresponding solvent; the spectra were taken at 3−5 min after the dissolution (22 °C). Typical spectra are shown in Figure S6, Supporting Information. [f] The isolated complex **1** (0.10 M) was dissolved in DMSO and then diluted 20-fold with H_2O; the spectrum was taken after 3−5 min (22 °C). Identical spectral parameters were observed for **1** in an aqueous buffer solution (1.0 mM Cr, 0.10 M HEPES, pH 7.4, Figure 9a).

hydroxamato complexes (a typical formula, $[Cr^{III}(LH)_3]^0$, in agreement with the literature data).[4a]

No evidence was obtained (from UV−vis spectroscopic or ESMS measurements) for the formation of Cr(IV) complexes of hydroxamic acids under the conditions that are known to stabilize Cr(IV) complexes with other types of ligands, including (i) the reactions of Cr(VI) with As(III) in weakly acidic aqueous media in the presence of excess ligand,[36] (ii) the reactions of Cr(VI) with hydroxamic acids in MeOH solutions,[7] (iii) the ligand-exchange reactions of hydroxamic acids with preformed Cr(IV) 2-hydroxycarboxylato complexes,[37] and (iv) the reactions of Cr(V) hydroximato complexes with one-electron reductants (thiols) in aqueous or DMF solutions.[38]

Synthesis and Characterization of a Cr(V)−BHA Complex, 1. A combination of EPR and UV−vis spectroscopies and ESMS was used to search for the reaction conditions that led to maximal yields of Cr(V) hydroximato complexes. Of all the studied ligands, the only complex to date that could be isolated in the solid state and purified by column chromatography was the Cr(V)−BHA complex (see the Experimental Section). Other complexes could be obtained in the solid state, but not in a pure form, and attempts to purify these complexes by column chromatography led to further decomposition of the complexes.

The purity of the isolated complex, **1**, was confirmed by the following methods: (i) ESMS (Figure 2, showing the absence of detectable amounts of Cr(VI) and Cr(III) species, by contrast with the crude reaction mixtures, Figure S3 and Table S1); (ii) solid-state EPR spectroscopy (Figure 3), showing the absence of Cr(III) species, which would lead to broad signals with $g \sim 2.0$ and $g \sim 4-5$;[9,10] (iii) IR spectroscopy (a comparison of spectra for **1** and the free ligand, BHA, is shown in Figure S4, Supporting Information); and (iv) magnetic susceptibility measurements (μ_{eff} = 2.07 μ_B at 295 K is within the range of values for well-characterized Cr(V) 2-hydroxycarboxylato complexes, 2.05−2.10 μ_B).[7,12] The presence of a Cr═O bond in **1** is supported by the observation of a band at 977 cm^{-1} in the IR spectrum (Figure S4).[35] The results of TGA (Experimental Section and Figure S5 in the Supporting Information) were consistent with the presence of one mole of acetone (which was used in the chromatographic purification of **1**) per mole of Cr. A characteristic signal due to acetone (ν(C═O), 1710 cm^{-1})[39] was evident in the IR spectrum of **1** (Figure S4), while several weaker peaks (e.g., 1360 and 1220 cm^{-1})[39] were obscured by those of the Cr(V) complex. The results of elemental analyses (Experimental Section) corresponded to the formulation of **1** as $K[Cr^VO(L)_2]\cdot Me_2CO$ (where LH_2 = BHA, Chart 1), except for the consistently lower than expected nitrogen contents (measured for three independent preparations of **1** in two laboratories). This discrepancy is likely to be due to the formation of CrN during the thermal

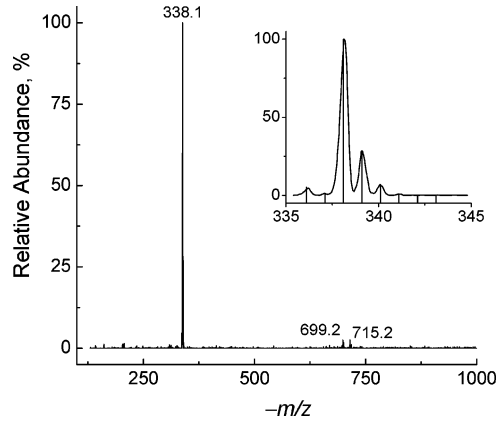

Figure 2. Typical ESMS data (negative-ion mode) for the isolated complex **1** (freshly prepared ~1.0 mM solution in acetone). No significant signals were observed in the positive-ion mode. Experimental (lines) and simulated (columns) isotopic distributions for the main signal are shown in the inset. Assignment of the signals (based on the *m*/*z* values and isotopic distribution patterns, LH_2 = BHA): $[Cr^VO(L)_2]^-$ (*m*/*z* = −338.1); $\{2[Cr^VO(L)_2]^-\cdot Na^+\}$ (*m*/*z* = −699.2); and $\{2[Cr^VO(L)_2]^-\cdot K^+\}$ (*m*/*z* = −715.2).

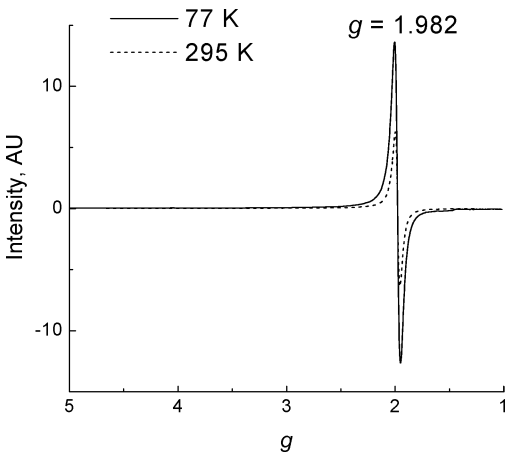

Figure 3. Solid-state X-band EPR spectra of **1** at 77 and 295 K.

(36) Ghosh, M. C.; Gould, E. S. *Inorg. Chem.* **1991**, *30*, 491−494.
(37) Codd, R.; Lay, P. A.; Levina, A. *Inorg. Chem.* **1997**, *36*, 5440−5448.
(38) Gould, E. S. *Coord. Chem. Rev.* **1994**, *135*, 651−684.
(39) Gordon, A. J.; Ford, R. A. *The Chemist's Companion. A Handbook of Practical Data, Techniques, and References*; John Wiley & Sons: New York, 1972; p 170.

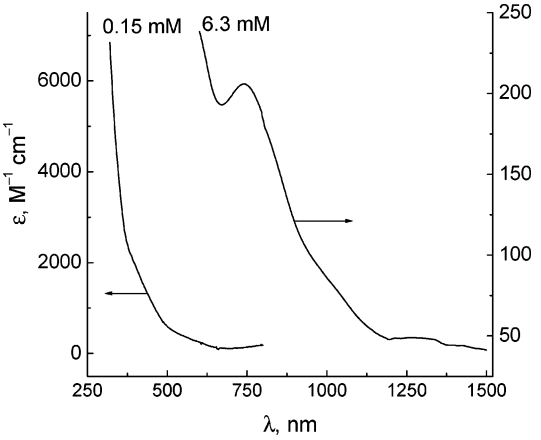

Figure 4. Electronic absorption spectra of **1** in DMF solutions (freshly prepared, 22 °C).

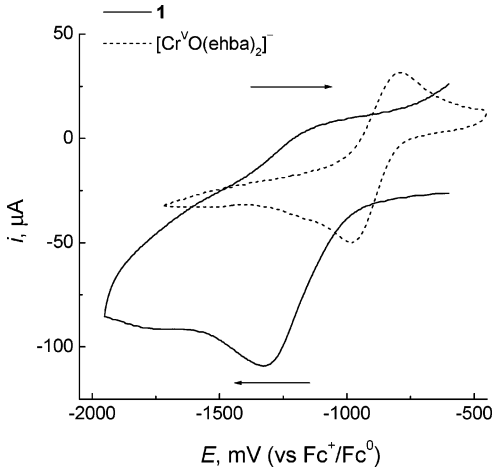

Figure 5. Typical cyclic voltammograms of **1** and $[Cr^{V}O(ehba)_2]^-$ ([Cr] = 5.0 mM) in DMF solutions (supporting electrolyte, 0.10 M $(^nBu_4N)BF_4$) on a glassy carbon electrode (diameter, 3 mm; scan rate, 100 mV s^{-1}). Directions of the scans are shown by arrows.

decomposition of **1**, by a process that is similar to the reaction described for Cr(III)−urea complexes.[40]

The electronic absorption spectra of **1** in polar organic solvents (e.g., DMF, Figure 4) possessed two poorly defined shoulders at 300−400 nm and 500−600 nm and a weak maximum at ∼740 nm ($\epsilon = 2.0 \times 10^2$ M^{-1} cm^{-1}), which is typical for Cr(V) complexes with O-donor ligands.[35]

Solution EPR spectra of **1** at 22 °C (Table 1 and Figure S6 in the Supporting Information) showed a strong solvent dependency of the line widths. The EPR signals of **1** in MeCN or acetone solutions were much broader than those in DMF or DMSO solutions, which led to poor resolution of the superhyperfine splitting patterns in the former two solvents (Figure S6). The other EPR spectral parameters (g_{iso}, A_{iso}, and a_N, Table 1) were not significantly solvent-dependent. Cyclic voltammetry of **1** in DMF solutions (using $(^nBu_4N)BF_4$ as a supporting electrolyte) showed irreversible reduction at $E = -1.33$ V (vs Fc^+/Fc^0, solid line in Figure 5), in contrast to a quasi-reversible Cr(V/IV) couple observed for $[Cr^{V}O(ehba)_2]^-$ under the same conditions ($E_{1/2} = -0.89$ V vs Fc^+/Fc^0, dashed line in Figure 5).[13] The maximal

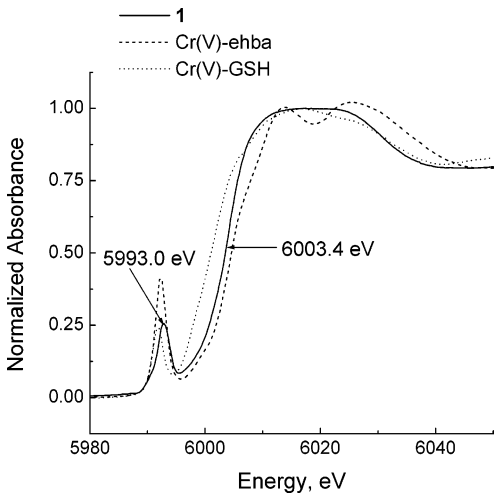

Figure 6. XANES spectrum of **1** in comparison with those of two previously characterized Cr(V) complexes: $Na[Cr^{V}O(ehba)_2]$ (Cr(V)−ehba)[42] and $Na_3[Cr^{V}O(LH_2)_2]$ (Cr(V)−GSH, LH_5 = GSH).[9] All the spectra were taken at 10 K from mixtures of the Cr(V) solids with BN.

cathodic current for the reduction of **1** was ∼2 times higher than the corresponding value for $[Cr^{V}O(ehba)_2]^-$ (at the same Cr concentration and scan rate, Figure 5), which points to a direct two-electron reduction of **1** to a Cr(III) complex. The reduction potential of **1** is comparable with those for Cr(V) peptide complexes ($E_{1/2} = -1.23$ to -1.34 V vs Fc^+/Fc^0 in DMF solutions),[41] but these complexes are reduced quasi-reversibly to Cr(IV) species.[41]

X-ray Absorption Spectroscopy of 1. The X-ray absorption near-edge structure (XANES) spectrum of **1** (Figure 6, solid mixture with BN, 10 K) shows a pre-edge absorbance peak typical for Cr(V) oxo complexes (due to a symmetry-forbidden $1s \rightarrow 3d$ transition that becomes allowed as a result of $d-p$ orbital mixing).[7−10,42] The edge position is shifted to lower energies by ∼1 eV compared with that of a typical Cr(V) complex with an *O*-donor ligand ($[Cr^{V}O(ehba)_2]^-$, Figure 6)[42] but is higher in energy by ∼2 eV compared with that for a Cr(V) complex with a *S*-/*N*-donor ligand ($[Cr^{V}O(LH_2)_2]^{3-}$, where LH_5 = GSH, Figure 6).[9]

SS modeling of the XAFS spectrum of **1** (typical results are listed in Table S2, Supporting Information) suggested the presence of one short (1.57 Å) and four longer (average length, 1.93 Å) Cr−O bonds in the first coordination shell of **1**, which is consistent with the proposed structure, $[Cr^{V}O(L)_2]^-$ (LH_2 = BHA, Chart 1). Models for MS XAFS analyses (Tables S3 and S4 in the Supporting Information) were built based on typical structures of five-coordinate Cr(V) oxo complexes[42] and on the geometric parameters of doubly deprotonated BHA ligands, determined by X-ray crystallography of Cr(III)−BHA complexes.[4] The models included all the non-H atoms that are likely to be found within 5 Å of the Cr atoms[20,24] (so that the three most distant C atoms in both Ph groups were truncated). The results of MS XAFS fittings for **1** and the optimized structure of the

(40) Qui, Y.; Gao, L. *J. Am. Ceram. Soc.* **2004**, *87*, 352−357.

(41) Barnard, P. J.; Levina, A.; Lay, P. A. *Inorg. Chem.* **2005**, *44*, 1044−1053.

(42) Levina, A.; Codd, R.; Foran, G. J.; Hambley, T. W.; Maschmeyer, T.; Masters, A. F.; Lay, P. A. *Inorg. Chem.* **2004**, *43*, 1046−1055.

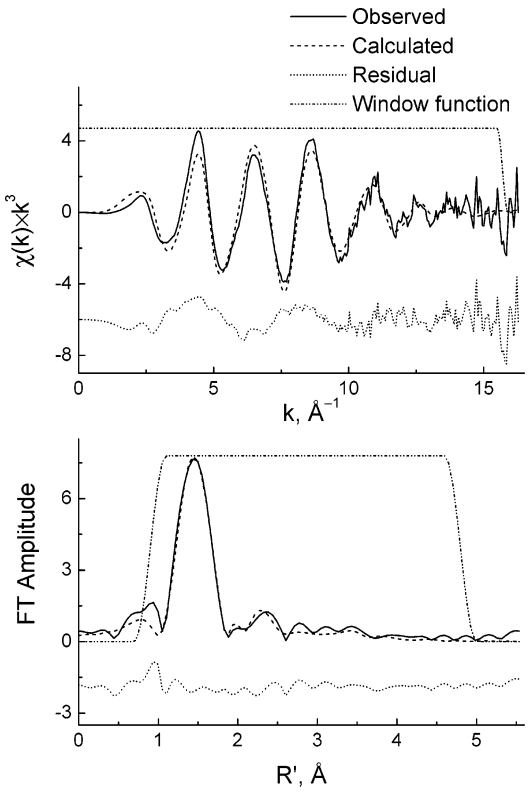

Figure 7. Experimental and calculated XAFS and Fourier transform (FT) XAFS spectra of **1** (solid, 10 K). The structure of the complex, optimized by MS XAFS calculations, is shown in Figure 8, and details of the MS XAFS calculations are given in Tables S3−S5, Supporting Information.

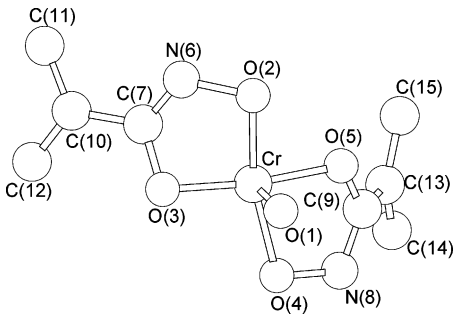

Figure 8. Structure of the complex **1**, optimized by MS XAFS calculations (the Ph groups of the ligands are truncated; calculation details are given in Tables S3−S5, Supporting Information). Selected parameters of the optimized model: |Cr−O(1)| = 1.58(2) Å; |Cr−O(2)| = |Cr−O(4)| = 1.98(2) Å; |Cr−O(3)| = |Cr−O(5)| = 1.88(2) Å; ∠O(1)−Cr−O(2) = ∠O(1)−Cr−O(4) = 82(2)°; ∠O(1)−Cr−O(3) = ∠O(1)−Cr−O(5) = 91(2)°; and ∠O(2)−Cr−O(3) = ∠O(4)−Cr−O(5) = 83(2)° (the values for equivalent bonds in both ligands were restrained to be equal within 0.02 Å or 2° during the calculations, Table S3). A full list of optimized parameters is given in Table S4 (model *trans*-**1**).

complex are shown in Figures 7 and 8, and details of the MS XAFS calculations are given in Tables S4 and S5, Supporting Information.

The initial models used for MS XAFS fitting to the structure of **1** included those with cis and trans positions of Ph groups relative to the Cr atom (similar to those in the X-ray crystal structures of Cr(III)−BHA complexes),[4] but the results of the best fits showed a clear preference for the trans models. This was based on better goodness-of-fit parameters (R = 14.4 vs 16.6% for the optimized trans and cis models, respectively, Table S4) and lower Debye−Waller factors for the atoms in the ligands (for the cis models, the latter values reached the upper limit of 0.02 Å^2, Table S4). The initial MS XAFS models had starting Cr−O bond lengths of 1.93 Å, which were chosen from the results of SS XAFS calculations (Table S3). However, all the unrestrained fits led to unequal Cr−O bond lengths, with longer bonds adjacent to the N atoms of the ligands (1.98(2) Å for Cr−O(2) and Cr−O(4) vs 1.88(2) Å for Cr−O(3) and Cr−O(5), Figure 8 and Table S4). Restrained models with the reversed order of Cr−O bond lengths or those with equal (within 0.02 Å) Cr−O bonds led to deterioration in the fits (the R values increased by 2−3%, Table S4), and calculations returned to the optimized model (Figure 8) when the restraints were released. The values of Cr═O bond lengths in **1**, optimized by MS XAFS fittings, were 1.57−1.58 Å (Table S4), in agreement with the SS XAFS results (Table S3). The optimized geometry of **1** (Figure 8 and Table S4) was close to those of typical distorted trigonal-bipyramidal structures of five-coordinate Cr(V) oxo complexes,[35,43] although MS XAFS calculations are unable, in most cases, to produce unique values of bond angles in metal complexes, due to relatively small MS contributions of the functional groups with bond angles at <150° (Table S5 in the Supporting Information).[24]

Reactivity of 1. Prolonged storage of **1** as a purified solid (~6 months at −20 °C, protected from light and moisture) led to a significant reduction of **1** to Cr(III) complexes, as determined by ESMS (Table S1) and column chromatography (Sephadex LH-20, see the Experimental Section). Solutions of **1** in aprotic solvents (1.0 mM in DMF, DMSO, MeCN, or acetone) were stable for at least 3 days at 22 °C (no significant decomposition was detected by EPR and UV−vis spectroscopies and ESMS), but repeated attempts to grow X-ray quality crystals of **1** from these solvents led to precipitation of Cr(III) complexes within several weeks or months, even at −20 °C. Solutions of **1** (1.0 mM) in MeOH or EtOH were completely reduced to Cr(III) complexes within ~12 h at 22 °C, as determined by EPR spectroscopy and ESMS.

Decomposition of **1** (0.20 mM) in aqueous solutions occurred over a time scale of seconds or minutes at 22 °C (as determined by EPR and UV−vis spectroscopies). The maximal lifetimes of the Cr(V) complexes were observed at pH ~ 7 (Table 2, the $t_{1/2}$ values apply only to [Cr] = 0.20 mM and are likely to be concentration-dependent). Formation of $[CrO_4]^{2-}$ (λ_{max} = 372 nm, $\epsilon_{max} = 4.81 \times 10^3$ M^{-1} cm^{-1})[44] during the decomposition of **1** in basic or neutral media (in the absence of added reductants) was evident from UV−vis spectra of the decomposition products (typical examples are shown in Figure S7, Supporting Information). The UV−vis spectra of the decomposition products of **1** in acidic media or in the presence of reductants, such as GSH, were consistent with the predominant formation of Cr(III) (a

(43) Lay, P. A.; Levina, A. In *Comprehensive Coordination Chemistry II*; McCleverty, J. A., Meyer, T. J., Eds.; Elsevier: Oxford, U.K., 2004; Vol. 4, pp 313−413.
(44) Brasch, N. E.; Buckingham, D. A.; Evans, A. B.; Clark, C. R. *J. Am. Chem. Soc.* **1996**, *118*, 7969−7980.

Table 2. Decomposition of **1** in Aqueous Solutions[a]

solution	$t_{1/2}$, s[b]	disproportionation, %[c]
H_2O (pH 6.6)	44	25
phosphate buffer (0.10 M, pH 7.4)	65	31
HEPES buffer (0.10 M, pH 7.4)	88	27
GSH (5.0 mM) in HEPES buffer (0.10 M, pH 7.4)	<5	0
acetate buffer (0.10 M, pH 4.0)	15	12
NaOH (0.10 M)	<5	41
HCl (0.10 M)	<5	5

[a] All the experiments were performed at [Cr] = 0.20 mM and 22.0 ± 0.1 °C. [b] The half-life time of **1** (0.20 mM) was measured by EPR and/or UV−vis spectroscopies. [c] The amount of **1** (mol %) decomposed by disproportionation (eq 2) was calculated from the concentration of Cr(VI) in the decomposition products (determined at $t \sim 10t_{1/2}$ by the DPC method),[16,17] using the known stoichiometry of Cr(V) decomposition (eqs 1 and 2).[46]

decrease in absorbance at 400−800 nm compared with the fresh solution of **1**, Figure S7).[9,10,45] Determination of Cr(VI) in the decomposition products (by the DPC method)[16,17] showed that **1** decomposes predominantly by ligand or substrate oxidation (eq 1) under all the conditions listed in Table 2. Typically for Cr(V) oxo complexes,[7,9,10,46] the role of disproportionation (eq 2) becomes more significant with an increase in the pH values of aqueous solutions (Table 2).

$$Cr(V)=O + S \rightarrow Cr(III) + S=O \quad \text{(S is the ligand or an added reductant)} \quad (1)$$

$$3Cr(V) \rightarrow 2Cr(VI) + Cr(III) \quad (2)$$

Studies by ESMS of the decomposition products of **1** in unbuffered H_2O (pH 6.6, reaction time 1 h at 22 °C) revealed the formation of $PhCOO^-$ as an oxidation product of BHA, as well as Cr(III)−BHA complexes and $[CrO_4]^{2-}$ (Figure S8 in the Supporting Information).

In a similar way as other Cr(V) oxo complexes,[9,10,33] **1** readily underwent ligand-exchange reactions with 1,2-diolato ligands, including D-glucose (a typical carbohydrate) or bovine mucin (a typical glycoprotein)[47,48] in neutral aqueous solutions, as shown by EPR spectroscopy (Figure 9). Dissolution of **1** (1.0 mM) in a weakly acidic solution (pH 4.0) containing a typical 2-hydroxycarboxylato ligand, $ehbaH_2$ (10 mM), led to the formation of $[Cr^VO(ehba)_2]^-$ (detected by EPR spectroscopy, $g_{iso} = 1.9783$, Figure S9 in the Supporting Information).[33] Estimation of equilibrium constants for these ligand-exchange reactions is complicated by the decomposition of **1**, which occurs over a similar time scale (Figures 9 and S9 and Table 2).

Biological Activity of 1. The data on the stability of **1** in aqueous solutions (Table 2) were used to design the conditions for testing of the biological activity of **1**. The ability of several types of Cr(V) complexes to induce oxidative DNA cleavage in vitro has led to the postulate that Cr(V) intermediates have an important role in Cr(VI)-induced

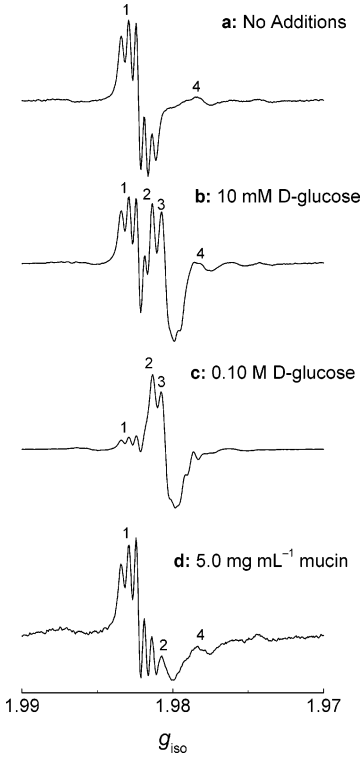

Figure 9. Typical X-band EPR spectra (solutions, 22 °C) for the ligand-exchange reactions of **1** (1.0 mM) with D-glucose or bovine mucin in HEPES buffers (0.10 M, pH 7.4); reaction time 3−4 min (a−c) or 8−10 min (d). The reaction solutions contained DMF (1% v/v) that was used for complete dissolution of **1**. Assignment of the signals: signal 1 ($g_{iso} = 1.9820$) is due to **1**, signal 2 ($g_{iso} = 1.9811$) is due to the mixed-ligand species (Cr(V)−BHA−carbohydrate), signal 3 ($g_{iso} = 1.9784-1.9805$) is due to Cr(V)−carbohydrate complexes (a mixture of linkage isomers),[33,47,48] and signal 4 ($g_{iso} = 1.9778$) is possibly due to a hydrolysis product of **1**.

genotoxicity and carcinogenicity.[5,49] In contrast to the activity of previously studied Cr(V) oxo complexes,[29,31,32,50−52] no significant cleavage of plasmid (pUC9) DNA was detected in aqueous solutions (phosphate buffers, pH 4.0−7.4) of **1** (0.20−1.0 mM) in the presence or absence of GSH (2.0 mM). Typical results of plasmid DNA cleavage assays for **1**, in comparison with those for the positive controls, $[Cr^VO(ehba)_2]^-$ [29,50] and $[Cr^V(O)_2(phen)_2]^+$,[10,32] are shown in Figure S10 (Supporting Information).

An additional nonoxidative pathway of Cr(V)-induced DNA damage, recently proposed for $[Cr^VO(ehba)_2]^-$,[30] involves the formation of Cr(III)−DNA adducts from reactive positively charged Cr(III) species (which readily bind to the negatively charged DNA backbone) that are formed during the decomposition of Cr(V) in neutral aqueous solutions. Incubation of **1** (0.50 mM) with fish sperm DNA (0.10 mg mL^{-1}) in HEPES buffer (0.10 M, pH 7.4, reaction time 1 h at 37 °C) caused relatively low levels of Cr−DNA binding (~2% of total Cr vs ~25% for $[Cr^VO(ehba)_2]^-$ under the same conditions).[30] Furthermore, no significant changes

(45) Lay, P. A.; Levina, A. *J. Am. Chem. Soc.* **1998**, *120*, 6704−6714.
(46) Krumpolc, M.; Roček, J. *Inorg. Chem.* **1985**, *24*, 617−621.
(47) (a) Codd, R.; Lay, P. A. *J. Am. Chem. Soc.* **2001**, *123*, 11799−11800. (b) Codd, R.; Lay, P. A. *Chem. Res. Toxicol.* **2003**, *16*, 881−892.
(48) Codd, R.; Irwin, J. A.; Lay, P. A. *Curr. Opin. Chem. Biol.* **2003**, *7*, 213−219.
(49) Sugden, K. D.; Stearns, D. M. *J. Environ. Pathol., Toxicol. Oncol.* **2000**, *19*, 215−230.
(50) Sugden, K. D.; Wetterhahn, K. E. *J. Am. Chem. Soc.* **1996**, *118*, 10811−10818.
(51) Sugden, K. D.; Campo, C. K.; Martin, B. D. *Chem. Res. Toxicol.* **2001**, *14*, 1315−1322.
(52) Levina, A.; Ludwig, C.; Lay, P. A. *J. Inorg. Biochem.* **2003**, *96*, 177.

in the levels of Cr−DNA binding were observed when **1** was allowed to decompose in the buffer solution (1 h at 37 °C, complete disappearance of Cr(V) was verified by EPR spectroscopy) prior to the addition of DNA (after which the reaction was continued for another 1 h at 37 °C). By contrast, decomposition of $[Cr^{V}O(ehba)_2]^-$ prior to the addition of DNA leads to a dramatic decrease in the levels of Cr−DNA binding, since the initially formed reactive Cr(III) species undergo base-catalyzed hydrolysis with the formation of nonreactive polynuclear complexes.[30] In summary, it appears that the Cr(III)−BHA complexes, formed during the decomposition of **1** in aqueous media (Figures S7 and S8), possess some DNA-binding ability, but this binding does not require the presence of Cr(V)−BHA species.

Bacterial mutagenicity assays with *S. typhimurium* (Ames tests)[53] are among the best-validated methods for the detection of chemical mutagens that include Cr(VI)[54] and several types of Cr(V) complexes.[29a,31,32] Preliminary results of these assays for fresh and decomposed (for 1 h at pH 7.4 and 37 °C) solutions of **1** (Table S6 in the Supporting Information) show that the observed weak effect of **1** is likely to be due to the formation of $[CrO_4]^{2-}$ (a known mutagen)[54] during the decomposition of **1** in neutral aqueous media, rather than due to a specific activity of the Cr(V) complex.

Discussion

Reactions of Cr(VI) with various hydroxamic acids in polar aprotic solvents led to relatively stable Cr(V)−hydroximato intermediates (detected by EPR and UV−vis spectroscopies and ESMS, Figures 1, S2 and S3), which represent a new family of Cr(V) compounds.[43] In these reactions, hydroxamic acids act as both reductants and ligands (in a similar manner as described for the syntheses of other Cr(V) complexes by the reactions of Cr(VI) with excess ligand).[9,12] The structures of the resultant complexes, $[Cr^{V}O(L)_2]^-$ (where LH_2 = hydroxamic acid, Chart 1), were assigned on the basis of the spectroscopic methods mentioned above. Their structures were confirmed by isolation and structural characterization (by MS analyses of XAFS spectroscopic data) of a Cr(V)−BHA complex, **1**, and the similarity of the EPR spectrum of this structurally characterized complex with the other complexes reported here. Notably, a Cr(V)−hydroximato complex was formed with high selectivity even with SaHA (as determined by EPR spectroscopy, Figure 1), a ligand that contains another strong donor group (phenolate). Thus, the hydroximato(2−) moiety provides a favorable coordination environment for Cr(V). By contrast, no stable Cr(IV)−hydroximato species were observed to date (see the Results). Irreversible electrochemical reduction of **1**, as well as the low reduction potentials (Figure 5), are consistent with very low stability of Cr(IV)−BHA species in solution. This difference in stabilities of Cr(V) and Cr(IV) complexes with hydroximato(2−) ligands parallels that for 1,2-diolato(2−) ligands[37] and is probably explained by the inability of Cr(IV) (a weaker electron acceptor than Cr(V))[37,38] to deprotonate the relatively weak acidic donor groups of the hydroxamic acids.

The proposed structures of Cr(V) hydroximato complexes, in which the O-donor atoms are adjacent to N atoms (Chart 1), are consistent with the observation of ^{14}N superhyperfine splitting in solution EPR spectra (Figure 1). The magnitude of the ^{14}N splitting ($\sim 0.9 \times 10^{-4}$ cm^{-1}, Table 1) was lower than that usually observed for N atoms bound directly to Cr(V) ($(2-3) \times 10^{-4}$ cm^{-1})[35,55] but similar to that for ^{1}H superhyperfine splitting due to the C−H bonds adjacent to the O-donor atoms in Cr(V) complexes with *cis*-diolato ligands.[33,35,48,55] The strength of the ^{14}N superhyperfine coupling can be explained by the spatial overlap of the d_{xy} orbital containing the unpaired electron with orbitals of the N atom in the chelate ring, in a similar manner as described for rationalizing the ^{1}H superhyperfine coupling of equatorial protons in the chelate rings of the interaction of the equatorial ring of *cis*-diolato ligands.[55]

Analyses of the XAFS spectrum of **1** (solid, 10 K), using MS models (Figure 7 and Tables S3−S5), suggested the dominance of a trans-isomer (Figure 8) in the solid state, which can be explained by the steric hindrance of the Ph residues in the ligands. Equilibrium mixtures of geometric isomers can be formed in solutions of **1** and other Cr(V)−hydroximato complexes, as such mixtures occur in the solutions of Cr(III)−hydroximato complexes[4] and of Cr(V) 2-hydroxycarboxylato complexes.[7,42] In a similar manner as that described for the well-studied Cr(V) 2-hydroxycarboxylato complexes (such as $[Cr^{V}O(ehba)_2]^-$), interconversions between the geometric isomers of **1** in solutions are likely to occur by intramolecular Berry twists.[35] The observed solvent-dependence of the line widths in the EPR signals (Table 1 and Figure S6) probably reflects the differences in the rates of Berry twists in various solvents. In the more polar solvents (DMF, DMSO, or H_2O), interconversions between the geometric isomers are fast on the EPR time scale, leading to narrow averaged signals (Table 1 and Figure S6). In the less polar solvents (MeCN or acetone), the rates of Berry twists in **1** become comparable with the EPR time scale, leading to the broadening of the signals (Table 1 and Figure S6).[35] The broadening of the outer ^{53}Cr satellite signals in the EPR spectra of Cr(V)−BHA species formed in situ in DMF solutions (Figure 1c) also suggests the presence of more than one geometric isomer in solution.[33,35]

A significant difference in the Cr−O(C) and Cr−O(N) bond lengths in **1** (1.88 and 1.98 Å, respectively, Figure 8), revealed by MS analyses of the XAFS data, is in contrast with the X-ray crystallographic data for Cr(III)−BHA complexes (*mer*-$[Cr^{III}(LH)_3]^0$ and *mer*- and *fac*-$[Cr^{III}(L)_3]^{3-}$, LH_2 = BHA), where these two types of bond lengths are similar (1.96−1.98 Å for Cr−O(C) and 1.95−1.96 Å for Cr−O(N)).[4b] These differences in bond lengths between the Cr(V) and Cr(III) complexes of the same ligand are likely to be due to the differences in geometry (distorted trigonal

(53) Maron, D. M.; Ames, B. N. *Mutat. Res.* **1983**, *113*, 173−215.
(54) Bennicelli, C.; Camoirano, A.; Petruzzelli, S.; Zanacchi, P.; De Flora, S. *Mutat. Res.* **1983**, *122*, 1−5.
(55) Codd, R.; Dillon, C. T.; Levina, A.; Lay, P. A. *Coord. Chem. Rev.* **2001**, *216−217*, 537−582.

bipyramidal vs octahedral) and the presence of a sterically demanding oxo group in the Cr(V) complex.

Like the Cr(V) 2-hydroxycarboxylato complexes[7,13] but unlike the Cr(V) complexes with amido or imine donor ligands,[10,31] the Cr(V) hydroximato complex, **1**, is much more stable in aprotic organic solvents (DMF, DMSO, MeCN, or acetone) than in aqueous media (see the Results). The reactivity patterns of **1** in aqueous solutions (Table 2), including a stability maximum at pH $\sim$ 7 and a predominant decomposition by a ligand-oxidation pathway (eq 1), are reminiscent of those for $[Cr^{V}O(LH_2)_2]^{3-}$ (where LH_5 = GSH).[9] Detailed mechanistic studies of the decomposition of **1** were beyond the scope of this work, particularly since our recent investigation of the decomposition of $[Cr^{V}O(ehba)_2]^{-}$ in aqueous solutions[56] showed a high degree of complexity of such reactions. Any comparisons of (i) the relative rates of reactions and (ii) the relative proportions of decomposition of **1** by competing disproportionation and ligand/solvent reduction reactions, compared with other Cr(V) complexes, cannot be related simply to the Cr(V/IV) reduction potential. Any analysis of such reactivity is complicated by the facts that (i) the reduction is irreversible in some cases (such as for **1**) but reversible in many others and (ii) there is a large range in the ease with which the coordinated ligand is oxidized. The very negative reduction potential combined with the relatively high proportion of ligand oxidation for **1** compared with other Cr(V) complexes, under the same conditions, suggests that it is the ease of ligand oxidation that is the main contribution to the lower stability of the complex compared with other bidentate chelating ligands such as 2-hydroxycarboxylates. Such an assertion is supported by the fact that **1** undergoes significant reduction to Cr(III) in the solid state (protected from moisture and light) over 6 months while most other Cr(V) solids with a variety of ligands are stable under these conditions. The relatively low stability of **1** in aqueous solutions (Table 2), combined with its very negative reduction potential (Figure 5), is probably responsible for its low reactivity toward DNA (Figure S10) and the absence of detectable mutagenicity in the TA102 strain of *S. typhimurium* (Table S6). This low biological activity of **1** is in stark contrast with the high mutagenicity and/or genotoxicity in vitro of many types of Cr(V) complexes, including those with 2-hydroxycarboxylato,[29,50] amido,[31] imine,[32,51] or thiolato (GSH)[52] donor ligands.

(56) Levina, A.; Lay, P. A.; Dixon, N. E. *Inorg. Chem.* **2000**, *39*, 385−395.

Chromium(V) hydroximato complexes are formed as unstable intermediates during the reactions of Cr(VI) with the ligands in neutral or weakly acidic aqueous media, as detected by EPR spectroscopy (Figure S1). Such complexes may also be formed during the microbial reduction of Cr(VI) in contaminated soils, due to the binding of Cr(V) to hydroximato ligands of siderophores, produced by soil bacteria or plants.[1,6] Once formed, such complexes could readily undergo ligand-exchange reactions with carbohydrate ligands (Figure 8), which are ubiquitous in biological systems, to form long-lived Cr(V) species.[48] In summary, a likely role of Cr(V) hydroximato complexes in biological systems is to serve as precursors of more stable and DNA-damaging species, such as Cr(V) carbohydrate complexes.

Acknowledgment. Financial support of this work was provided by Australian Research Council (ARC) Large and Discovery grants and an Australian Professorial Fellowship to P.A.L., ARC RIEFP for the 10-element Ge detector, Wellcome Trust and ARC RIEF grants for the ESMS and EPR equipment, and Australian Synchrotron Research program (ASRP) grants for access to the Australian National Beamline Facility (ANBF) in Tsukuba, Japan. The X-ray absorption spectroscopic (XAS) studies were performed at ANBF with support from the ASRP, which is funded by the Commonwealth of Australia under the Major National Research Facilities program. R.C. is grateful for funding through the Gritton Postdoctoral Fellowship. We thank Drs. Garry Foran (ANBF) and Hugh Harris (University of Sydney) for assistance in recording the XAS data, Professor Nicholas Dixon and Mrs. Penelope Lilley (Australian National University) for providing pUC9 plasmid DNA, Dr. Antonio M. Bonin (University of Sydney) for providing the *Salmonella* strain and assistance with the bacterial mutagenicity assays, and Dr. Colin L. Weeks (University of Sydney) for assistance with TGA.

Supporting Information Available: Tables showing the assignment of major ESMS signals observed during the reactions of Cr(VI) with hydroxamic acids, details of SS and MS XAFS calculations, and typical results of *Salmonella* mutagenicity assays; and Figures showing typical spectroscopic data (EPR, UV−vis, and ESMS) for the reactions of Cr(VI) with hydroxamic acids, and detailed characterization of **1**, including IR spectra, TGA data, EPR spectra in various solvents, UV−vis spectra and ESMS data for decomposed aqueous solutions, and typical results of DNA cleavage assays in comparison with those for other Cr(V) complexes. This material is available free of charge via the Internet at http://pubs.acs.org.

IC048317D